

Structural properties and charge-ordering transition in $\text{LaSr}_2\text{Mn}_2\text{O}_7$

J. Q. Li and Y. Matsui

National Institute for Research in Inorganic Materials, 1-1 Namiki, Tsukuba, Ibaraki 305, Japan

T. Kimura

Joint Research Center for Atomic Technology, Tsukuba, 305, Japan

Y. Tokura

*Joint Research Center for Atomic Technology, Tsukuba, 305, Japan
and Department of Applied Physics, University of Tokyo, Tokyo 113, Japan*

(Received 22 July 1997; revised manuscript received 29 September 1997)

Transmission-electron-microscopy measurements characterizing the structure and charge-ordered states in $\text{LaSr}_2\text{Mn}_2\text{O}_7$ are presented. The crystal structure of this phase has been identified as a well-defined 327 layered structure by high-resolution electron microscopy and image simulation. Electron diffraction reveals at low temperature the presence of additional superstructure spots along the $[110]$ direction. This superstructure is interpreted in terms of the charge ordering of Mn^{3+} and Mn^{4+} associated with the d_{z^2} orbital ordering of Mn^{3+} . Possible ordering models are proposed. [S0163-1829(98)50906-X]

The discovery of colossal magnetoresistance (CMR) in perovskite manganites $R_{1-x}A_x\text{MnO}_3$ (R and A being trivalent rare-earth and divalent alkaline-earth ions, respectively) has stimulated considerable interest in the study of physical and structural properties of the related systems.¹⁻³ Recently, distinct phases in the layered perovskite family $(\text{La,Sr})_{n+1}\text{Mn}_n\text{O}_{3n+1}$ with $n=1, 2$, and ∞ have been prepared and studied. The basic structure in this homologous series appears to be based on alternate stacking of rock-salt-type block layers $(\text{La,Sr})_2\text{O}_2$ and MnO_2 sheets along the c -axis direction. Higher members in this family can be obtained by intercalation of the $(\text{La,Sr})\text{O}-\text{MnO}_2$ bilayers. The measurements of magnetic susceptibility and electronic transport revealed a number of special phenomena in this system,^{4,5} e.g., a very high CMR effect was observed in $(\text{La}_{0.4}\text{Sr}_{0.6})_3\text{Mn}_2\text{O}_7$ with a nominal hole concentration $x=0.4$, and a charge-ordering (CO) transition was evident in $\text{LaSr}_2\text{Mn}_2\text{O}_7$ ($x=0.5$).⁶ In fact, the interplay of charge, lattice, and spins in the layered system has attracted substantial attention in present studies. In this Communication, we report the structural properties and the charge-ordered states in $\text{LaSr}_2\text{Mn}_2\text{O}_7$ as revealed by transmission electron microscopy.

Single crystalline samples of $\text{La}_{2-2x}\text{Sr}_{1+2x}\text{Mn}_2\text{O}_7$ were melt-grown by the floating-zone (FZ) method. The detailed process of the sample preparation has been described in Refs. 4-6. At low temperature, the samples were found to be conducting ferromagnets for $0.3 \leq x \leq 0.4$ as reported previously. However, from the measurements of transport and magnetic susceptibility, a CO transition was evident in $\text{LaSr}_2\text{Mn}_2\text{O}_7$ with $x=0.5$. The resistivity data shows a jumplike increase at the transition temperature $T_{\text{co}} \approx 210$ K. X-ray diffraction measurements showed that the single crystalline samples have the tetragonal structure with the space group $I4/mmm$ at room temperature. Furthermore, the quality of $\text{La}_{2-2x}\text{Sr}_{1+2x}\text{Mn}_2\text{O}_7$ ($0 \leq x \leq 0.5$) single crystalline samples were checked by inductively coupled plasma atomic emis-

sion spectroscopy; the results indicated that they are nearly stoichiometric. Thin samples for electron diffraction and high-resolution electron microscopy (HREM) studies were prepared simply by crushing the $\text{LaSr}_2\text{Mn}_2\text{O}_7$ material into fine fragments with CCl_4 , which were then dispersed on Cu grids coated with wholly carbon support films. A Hitachi H-1500 transmission-electron microscope equipped with a low-temperature sample stage was used for the present studies.

The $\text{LaSr}_2\text{Mn}_2\text{O}_7$ single-crystalline sample was first characterized at room temperature. The resultant HREM and electron diffraction data indicated that the $\text{LaSr}_2\text{Mn}_2\text{O}_7$ phase has a well-defined 327-type layered structure. Figure 1 shows a HREM image taken along the $[100]$ zone-axis direction. This image was obtained from a thin region of the crystal under the defocus value around the Scherzer defocus (~ -60 nm). The metal atom positions are therefore recognizable as dark dots. The layered structure of the

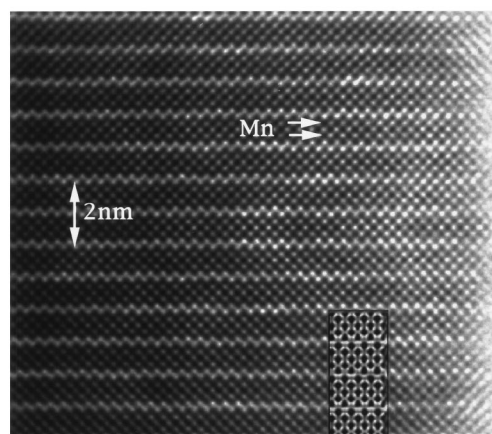


FIG. 1. High resolution image of $\text{LaSr}_2\text{Mn}_2\text{O}_7$ taken along the $[100]$ direction. A simulated image is superimposed onto the experimental image.

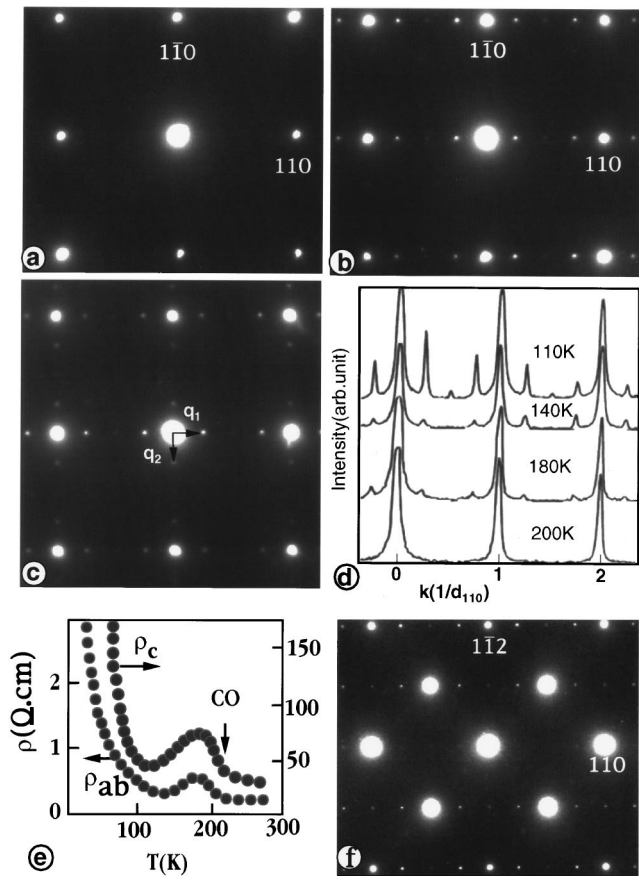


FIG. 2. [001] zone-axis electron diffraction patterns of $\text{LaSr}_2\text{Mn}_2\text{O}_7$ obtained at (a) 300 K and (b) 110 K, respectively. The presence of superlattice reflections at low temperature is evident. (c) Diffraction pattern exhibiting the presence of 90° twin domain at 110 K. (d) Microphotometric density curves along the a^*+b^* direction showing the temperature variation of the superlattice reflections. (e) Temperature dependence of the resistivity of $\text{LaSr}_2\text{Mn}_2\text{O}_7$. (f) $[\bar{1}11]$ zone-axis diffraction pattern (i.e., tilted about 15° from the [001] zone axis). Note that the satellite spots along the principal $[hh0]$ direction are almost absent.

$\text{LaSr}_2\text{Mn}_2\text{O}_7$ phase along the c direction can be clearly read out in this macrograph. Image calculations based on the structural models proposed previously^{4,5} were carried out by varying the crystal thickness from 2 to 5 nm and the defocus value from -50 to -65 nm. A calculated image for a defocus value of -60 nm and a thickness of 2.5 nm, superimposed onto the image, appears to be in good agreement with the experimental one. It should be noted that in this single-crystal sample no intergrowth of the other phases, such as $\text{La}(\text{Sr})\text{MnO}_2$ and $\text{La}(\text{Sr})_2\text{MnO}_4$, has been found, while such intergrowth defects were commonly observed in polycrystalline samples.

We now focus on the low-temperature investigation of the CO transition in the $\text{LaSr}_2\text{Mn}_2\text{O}_7$ material. The diffraction evidence for a CO transition is given by the presence of additional superstructure reflections in the diffraction patterns obtained at low temperatures. Figures 2(a) and 2(b) show the [001] zone-axis electron diffraction patterns of $\text{LaSr}_2\text{Mn}_2\text{O}_7$ taken, respectively, at room temperature and 110 K. The diffraction pattern at room temperature has been

indexed with the known $I4/mmm$ tetragonal structure with lattice parameters $a=b=0.385$ nm and $c=1.98$ nm. The most striking feature revealed in Fig. 2(b) is the appearance of a series of sharp satellite spots in addition to the fundamental Bragg reflections. The wave vector of this structural modulation was found to be commensurate and can be written as $\mathbf{q}=\mathbf{a}^*[\frac{1}{4},\frac{1}{4},0](\mathbf{a}\cdot\mathbf{a}^*=1)$. Upon cooling from room temperature, the superstructure reflections normally become visible just below ~ 200 K. Because of the heating effect and due to the dynamical nature of the electron scattering, a precise measurement of the transition temperature is difficult in the present case. Sometimes, two sets of superstructure reflections appear around each basic Bragg spot as shown in Fig. 2(c), in which two sets of superstructure reflections are indicated by \mathbf{q}_1 and \mathbf{q}_2 , respectively. These two sets of superstructure spots are considered to originate from the twin domains where the superstructure vectors are rotated by 90° with respect to one another. This kind of twin domain was previously observed and reported in other related systems.^{7,8} The temperature dependence of the superstructure reflections has also been investigated from room temperature (300 K) down to 110 K. Normally, the weak satellite reflections become visible at around 200 K, and then the intensities of the superstructure spots increase progressively with decreasing temperature. The microphotometric density curves measured along the a^*+b^* direction are shown in Fig. 2(d), which clearly demonstrates the increase of the intensities of the superstructure peaks at lower temperature. No significant change of the periodicity of the CO modulation with temperature has been found in our experiments.

From measurements of transport and magnetic susceptibility, the CO transition has been assumed to be induced at around 210 K. In Fig. 2(e), a typical result of measurements of the temperature dependence of the resistivity is described, in which an anomalous behavior at around 210 K is clearly evident. The detection of the superstructure reflections at low temperatures provides a direct structural evidence for this CO transition. We now proceed to determine the basic characteristics of the superstructure modulation in the $\text{LaSr}_2\text{Mn}_2\text{O}_7$ phase. It was found that the satellite spots at $(h\pm\frac{1}{4},h\pm\frac{1}{4},0)$ were very weak in some cases, and their intensities decreased very rapidly as the sample was tilted away from the [001] zone axis. A typical diffraction pattern taken along the $[\bar{1}11]$ zone-axis direction is shown in Fig. 2(f) in which the superlattice spots at the systematic positions $(h,h,0)\pm m\mathbf{q}$ almost disappear. This observation indicates that the superlattice reflections at $(h,h,0)\pm m\mathbf{q}$ positions are caused by double reflection. Careful study of diffraction patterns with various orientations indicates that the superstructure reflections are absent in the $(110)^*$ section of the reciprocal space. This fact suggests that a pure transverse lattice distortion has been induced in the $\text{LaSr}_2\text{Mn}_2\text{O}_7$ crystal lattice by the CO transition.⁹

In $\text{LaSr}_2\text{Mn}_2\text{O}_7$ there are as many $\text{Mn}^{4+}(3d^3)$ as $\text{Mn}^{3+}(3d^4)$ ions, and therefore the CO model, originally proposed by Goodenough¹⁰ for the cubic perovskite $\text{La}_{0.5}\text{M}(\text{II})_{0.5}\text{MnO}_3$, can be used in principle to explain our experimental results. In Goodenough's model, the CO between Mn^{3+} and Mn^{4+} is accompanied by the ordered arrangements of the $d_{z^2}(\text{Mn}^{3+})$ orbital orientations to form the zigzag chains in the basic plane. In the present case, the

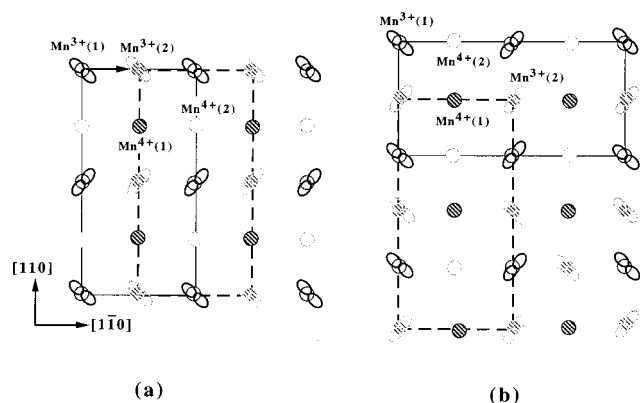


FIG. 3. Schematic representations of possible charge- and orbital-ordered states projected along the [001] direction. In order to simplify the drawing, only the Mn³⁺ and Mn⁴⁺ ions are shown: (a) a model with the stacking translation vector $R = (\frac{1}{2}, -\frac{1}{2}, 0)$ as indicated by an arrow; (b) a typical 90° twin domain.

LaSr₂Mn₂O₇ phase has a layered structure with the space group $I4/mmm$, which results in a relative shift between the neighboring layers in the CO patterns. In Figs. 3(a) and 3(b), two models of ionic ordering of Mn⁴⁺ ($3d^3$) and Mn³⁺ ($3d^4$) are shown, both of which are in agreement with the charge-ordered states observed at low temperature. In addition to Mn⁴⁺-Mn³⁺ ionic ordering, the superstructure with the periodicity of $L = 4d_{110}$ along the $a^* + b^*$ direction is produced by the orientational ordering of the $d_{z^2}(\text{Mn}^{3+})$ orbital. It should be noted that the structural model in Fig. 3(a) only represents the projection of the charge-ordered state in LaSr₂Mn₂O₇ along the [001] direction, with a stacking vector $R = (\frac{1}{2}, -\frac{1}{2}, 0)$ as indicated by an arrow. The stacking of the successive charge (orbital) ordered arrangements between the layers could also be offset by several other stacking vectors, e.g., $R = (\frac{1}{2}, \frac{1}{2}, 0)$. Here we only present those models which appear to be experimentally acceptable. Figure 3(b) shows the model of a typical 90° twin domain, which is assumed to be induced by the rotation of the CO modulations between the neighboring layers and frequently observed in the electron diffraction investigations, as mentioned above. In this case the twin boundary is located in the plane between the La(Sr)-O layers. For checking the correctness of our models, we have carried out theoretical simulations. Unfortunately, so far no neutron diffraction data has been reported about the structural changes with the CO transition in the LaSr₂Mn₂O₇ phase. Based on our results in combination with the neutron diffraction data for La_{0.5}Ca_{0.5}MnO₂ (Ref. 11) and La_{0.5}Sr_{1.5}MnO₄ (Ref. 12), we have obtained qualitative results, which result in the diffraction patterns with reflection conditions in agreement with the experimental ones. However, the intensity of the satellite spots was found to be very sensitive to the displacement of Mn⁴⁺ ions, therefore better results can be expected from theoretical simulations based on the neutron diffraction results on this CO transition.

In addition to the CO transition, the CO incommensurability is another main question investigated in manganites.⁷ In fact, the electron diffraction observation revealed at low temperature that the structural modulation is incommensurate in some grains. Figure 4(a) shows a typical electron

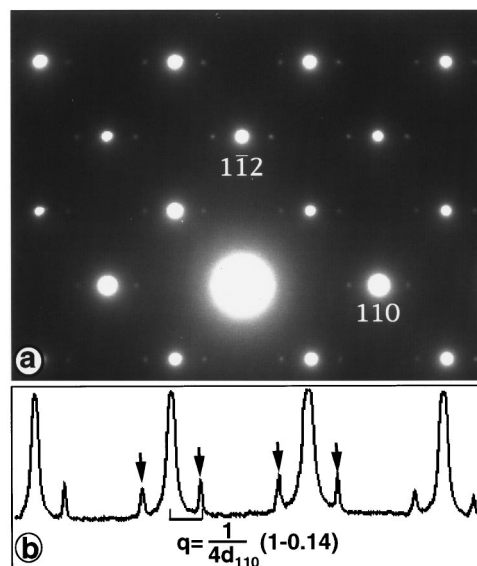


FIG. 4. (a) Electron diffraction pattern obtained at 110 K; the presence of incommensurate satellites is evident. (b) Microphotometric density curve along the $a^* + b^*$ direction clearly shows the incommensurability of the satellite reflections.

diffraction pattern exhibiting an incommensurate modulation along the $a^* + b^*$ direction. The wave vector of the CO modulation in the present case can be expressed as $q \approx (\frac{3}{14}, \frac{3}{14}, 0) \sim (1/4d_{110})(1-0.14)$, which results in the incommensurability parameter $\delta = 0.14$. Figure 4(b) shows the microphotometric density curve along the $a^* + b^*$ direction, in which the incommensurate peaks are clearly indicated. It is also found that the incommensurability parameter does not change distinguishably with increasing of temperature, until the superstructure reflections become invisible at around 200 K. Hence, the incommensurability in the present case is probably due to the local inhomogeneity of chemical composition, e.g., the inhomogeneous distribution of Sr as well as O ions in the sample.

Considering the large intensity of the superstructure spots at low temperature (below 140 K), we can conclude that the local structure in the charge-ordered phase significantly deviates from the average structure. Analyses of the diffraction patterns and the satellite spots obtained for various temperature ranges indicate that at low temperature the structure of LaSr₂Mn₂O₇ is one-dimensionally modulated. The average structure has an orthorhombic (or pseudotetragonal) unit cell, with the lattice parameters $a_0 \cong b_0 = 0.545$ nm and $c_0 \cong 1.96$ nm. For analyzing the CO modulation in the way suggested by De Wolff *et al.*,¹³ we require four basis vectors in the reciprocal space to describe both the main spots and the satellite spots. Therefore, a fourth index m and the corresponding reciprocal basis vector $\mathbf{Q} = \alpha \mathbf{a}_0^*$ ($\alpha = 0.5 - \varepsilon$) have been introduced. The reciprocal lattice vector \mathbf{H} for the CO phase can then be expressed as $\mathbf{H} = H\mathbf{a}_0^* + K\mathbf{b}_0^* + L\mathbf{c}_0^* + m\mathbf{Q}$, where H , K , L , and m are integers.

The systematic extinction conditions associated with this one-dimensionally modulated structure is observed to be $H + L + K = 2n$ in general; $H = 2n$ ($K = 2n$) for $(HK0)$; $K + L = 2n$ for $(0KL)$; $L + H = 2n$ for $(H0L)$.

From the general reflection condition verified by all of the reflections, we can conclude that the four-dimensional super-

space group belongs to the Bravais class P_{111}^{Immm} (No. 12).¹³ Whereas the other special conditions are nonprimitive, the superspace group of the CO phase in $\text{LaSr}_2\text{Mn}_2\text{O}_7$ can be determined uniquely as P_{111}^{Imma} . This would result in the space group for the average structure as $Imma$, choosing the origin as proposed in Ref. 14.

In summary, the crystal structure of the $\text{LaSr}_2\text{Mn}_2\text{O}_7$ phase has been identified by HREM as a well-defined 327-type layered structure. At low temperature, electron diffraction observations directly reveal the presence of extra superstructure reflections distributed along the $a^* + b^*$ direction. In most grains this superstructure modulation is found to be commensurate, with a wave vector $\mathbf{q} = [\frac{1}{4}, \frac{1}{4}, 0]$, which can be

understood in terms of charge and orbital ordering in $\text{LaSr}_2\text{Mn}_2\text{O}_7$. The possible ordering schemes, based on the separation of Mn^{3+} and Mn^{4+} into two interpenetrating commensurate sublattices and accompanied by a d_{z^2} (Mn^{3+}) orbital ordering, have been proposed as the possible interpretations of our observations. The superspace group of charge-ordered state in $\text{LaSr}_2\text{Mn}_2\text{O}_7$ is determined uniquely as P_{111}^{Imma} .

The authors would like to express many thanks to C. Tsutsumi for his assistance. The work reported here was in part supported by the COE project organized by the Science and Technology Agency, and by the New Energy and Industrial Technology Development Organization (NEDO), Japan.

-
- ¹K. Chabara, T. Ohno, M. Kasai, and Y. Kozono, *Appl. Phys. Lett.* **63**, 1990 (1993).
- ²R. von Helmolt, J. Wecker, B. Holzapfel, L. Schultz, and K. Samwer, *Phys. Rev. Lett.* **71**, 2331 (1993).
- ³Y. Tokura, A. Urushibara, Y. Moritomo, T. Arima, A. Asamitsu, G. Kido, and N. Furukawa, *J. Phys. Soc. Jpn.* **63**, 3931 (1994).
- ⁴Y. Moritomo, A. Asamitsu, H. Kuwahara, and Y. Tokura, *Nature (London)* **380**, 141 (1996).
- ⁵T. Kimura, Y. Tomioka, H. Kuwahara, A. Asamitsu, M. Tamura, and Y. Tokura, *Science* **274**, 1698 (1996).
- ⁶T. Kimura and Y. Tokura (unpublished).
- ⁷C. H. Chen *et al.*, *Phys. Rev. Lett.* **76**, 4042 (1996).
- ⁸Y. Moritomo, Y. Tomioka, A. Asamitsu, Y. Tokura, and Y. Matsui, *Phys. Rev. B* **51**, 3297 (1995).
- ⁹J. Van Landuyt, G. Van Tendeloo, and S. Amelinckx, *Phys. Status Solidi A* **26**, K9 (1974).
- ¹⁰J. B. Goodenough, *Phys. Rev.* **100**, 564 (1955).
- ¹¹P. G. Radaelli, D. E. Cox, M. Marezio, and S.-W. Cheong, *Phys. Rev. B* **55**, 3051 (1997).
- ¹²B. J. Sternlieb, J. P. Hill, and U. C. Wildgruber, *Phys. Rev. Lett.* **76**, 2169 (1996).
- ¹³P. M. De Wolff, T. Janssen, and A. Janner, *Acta Crystallogr., Sect. A: Cryst. Phys., Diffr., Theor. Gen. Crystallogr.* **37**, 625 (1981).
- ¹⁴N. F. H. Henry and K. Lonsdale, *International Table for X-ray Crystallography* (Kynoch, Birmingham, 1969), Vol. 1.